AFRL-PR-WP-TR-2006-2175

SHOCKWAVE PROPAGATION IN NONEQUILIBRIUM AIR PLASMA

Biswa N. Ganguly

Electrical Technology & Plasma Physics Branch (AFRL/PRPE)
Power Division
Propulsion Directorate
Air Force Materiel Command, Air Force Research Laboratory
Wright-Patterson Air Force Base, OH 45433-7251

JULY 2006

Final Report for 25 February 1997 – 01 July 2006

PROPULSION DIRECTORATE
AIR FORCE MATERIEL COMMAND
AIR FORCE RESEARCH LABORATORY
WRIGHT-PATTERSON AIR FORCE BASE, OH 45433-7251

NOTICE

PAO case number: AFRL/WS 06-1654
Date cleared: 05 Jul 2006

THIS TECHNICAL REPORT IS APPROVED FOR PUBLICATION.

//Signature//

BISWA N. GANGULY
Principal Research Physicist
Electrical Technology &
Plasma Physics Branch

//Signature//

JOSEPH A. WEIMER
Chief
Electrical Technology &
Plasma Physics Branch

//Signature//

KIRK L. YERKES, PhD
Deputy for Science
Power Division

REPORT DOCUMENTATION PAGE

Form Approved
OMB No. 0704-0188

1. REPORT DATE *(DD-MM-YY)*	2. REPORT TYPE	3. DATES COVERED *(From - To)*
July 2006	Final	02/25/1997 – 07/01/2006

4. TITLE AND SUBTITLE
SHOCKWAVE PROPAGATION IN NONEQUILIBRIUM AIR PLASMA

5a. CONTRACT NUMBER
In-house

5b. GRANT NUMBER

5c. PROGRAM ELEMENT NUMBER
61102F

6. AUTHOR(S)
Biswa N. Ganguly

5d. PROJECT NUMBER
2308

5e. TASK NUMBER
BW

5f. WORK UNIT NUMBER
00

7. PERFORMING ORGANIZATION NAME(S) AND ADDRESS(ES)

Electrical Technology & Plasma Physics Branch (AFRL/PRPE)
Power Division
Propulsion Directorate
Air Force Materiel Command, Air Force Research Laboratory
Wright-Patterson Air Force Base, OH 45433-7251

8. PERFORMING ORGANIZATION REPORT NUMBER
AFRL-PR-WP-TR-2006-2175

9. SPONSORING/MONITORING AGENCY NAME(S) AND ADDRESS(ES)

Propulsion Directorate
Air Force Research Laboratory
Air Force Materiel Command
Wright-Patterson AFB, OH 45433-7251

10. SPONSORING/MONITORING AGENCY ACRONYM(S)
AFRL-PR-WP

11. SPONSORING/MONITORING AGENCY REPORT NUMBER(S)
AFRL-PR-WP-TR-2006-2175

12. DISTRIBUTION/AVAILABILITY STATEMENT
Approved for public release; distribution is unlimited.

13. SUPPLEMENTARY NOTES

14. ABSTRACT

The effects of acoustic shock wave propagation in nonequilibrium plasmas with Mach number from 1.5 up to 2.5 have been investigated. The effects of shock wave induced double layer on local excitation and ionization enhancement have been measured. Also, the effect of local gas heating induced by the energy dissipation in the double layer has been measured in a dielectric barrier discharge.

15. SUBJECT TERMS
shock wave, plasma physics, dielectric barrier discharge, optical spectroscopy

16. SECURITY CLASSIFICATION OF:			17. LIMITATION OF ABSTRACT:	18. NUMBER OF PAGES	19a. NAME OF RESPONSIBLE PERSON (Monitor)
a. REPORT	b. ABSTRACT	c. THIS PAGE			Biswa N. Ganguly
Unclassified	Unclassified	Unclassified	SAR	46	19b. TELEPHONE NUMBER *(Include Area Code)* N/A

Standard Form 298 (Rev. 8-98)
Prescribed by ANSI Std. Z39-18

Shockwave Propagation in Nonequilibrium Air Plasma

Biswa N. Ganguly

AFRL/PRPE

Abstract

The effects of acoustic shock wave propagation in nonequilibrium plasmas with Mach number from 1.5 up to 2.5 have been investigated. The effects of shock wave induced double layer on local excitation and ionization enhancement have been measured. Also, the effect of local gas heating induced by the energy dissipation in the double layer has been measured in a dielectric barrier discharge.

Acknowledgement: This work was performed in collaboration with Drs. Peter Bletzinger and Alan Garscadden.

1. **Introduction**

To reduce drag, the high speed vehicle profile has a narrow cone angle; however, this geometry makes active cooling difficult. Progress in vehicle design and in materials had matured at the beginning of the 1990s so it was with considerable enthusiasm that plasma – thermal mechanisms to reduce drag have been investigated in Russia and more recently, in the West. A number of imaginative schemes were proposed to modify and control the flow around a hypersonic vehicle. These schemes included novel approaches for plasma generation, MHD flow control and power generation and new hot gas counter-flows and other purely thermal approaches.

The first experiments were in a ballistic tunnel where relatively small projectiles at hypersonic velocities traveled through partially ionized plasmas. Less expensive experiments which permitted close examination of the plasma environment have used positive column plasmas, radio-frequency and microwave – excited discharges. Other studies have used plasma jets, corona plasmas and laser-generated plasmas to modify the shock ahead of the test object in a wind tunnel.

These studies led to much stronger interactions between researchers in the former Soviet Union (FSU), USA and European groups. To promote communication, notable series of meetings were started. The first meeting series are held each spring on "Perspectives of MHD and Plasma Technologies in Aerospace Applications" and are held in the FSU. The second series of meetings are the so-called Weakly Ionized Gas

(WIG) meetings which are now special sessions at the annual American Institute of Aeronautics and Astronautics Aerospace Sciences meeting.

The introduction of plasma into high-speed aerodynamic flowfields with their inherent strong gradients resulted in a fascinating array of physical processes including the complex interactions that occur at shock waves. A review of these processes is provided in the following sections. As will be seen, separating the effects of the various physical processes that generally occur simultaneously represents a significant challenge in many experiments. For example, to sort out the different effects of plasma on a shock wave and also of the shock on the plasma, ideally one would perform experiments in the same configuration for several rare gases and for several molecular gases. The fractional power that goes into gas heating can be calculated and measured reasonably accurately for the pure gases. Gas heating at the same current density is a lot larger in diatomic gases like nitrogen or air than in argon and one would expect that the shock characteristics would change correspondingly. In more complex polyatomic gases like carbon dioxide and sulfur hexafluoride, the internal energy relaxation times are shorter then in nitrogen, and if internal energy release were critical, the measurements should show the effect.

Also, it is more difficult to obtain uniform discharges in molecular gases than in rare gases. Then the question is how much does plasma uniformity matter in the reduction of drag and the attenuation of the shock. If the effects are just thermal energy deposition with no particular leverage of the effects of the shock wave on the plasma, then one must ask is there any leverage from the position of the plasma induced thermal disturbance.

These and other issues associated with plasma creation in high speed airflows are reviewed in the following experiments.

2. Evidence of enhanced electronic excitation at the shock front of low Mach number shocks in non-equilibrium plasmas

The propagation and dispersion of weak shock waves in non-equilibrium plasmas have recently received considerable attention [1-6]. Optical and pressure probe measurements show spreading of the shock front and an increase in shock velocity in the plasma. Some investigators relate these effects to axial or radial thermal gradients[4,5] in the plasma, others invoke effects caused by a shock wave induced electrostatic interactions [1,3] in the plasma. Depending on the boundary conditions of the experiments, these interpretations may be applicable. We have recently investigated [6] the interaction of the shock wave with the N_2 plasma in a DC glow discharge and have shown that the propagating shock wave causes large local changes in the electric field in the immediate vicinity of the shock front as well as global changes in discharge voltage and current. The magnitudes of these effects were shown to be dependent on discharge polarity. Spatially and temporally resolved measurements of the optical emission from the $C^3\Pi_u$ - $B^3\Pi_g$ transition in nitrogen showed sharp decreases when the shock wave passed through the observation point. Fig.1 shows a series of ICCD camera images taken with a 1.2 μs exposure time and a blue filter, which eliminates the emission of the nitrogen recombination afterglow. The ICCD pictures were made on a 5 cm diameter, 5 Torr, 60 mA discharge.

As the shock wave sweeps through the positive column, the discharge becomes dark behind the shock. This result indicates a significant decrease in the reduced electric field

E/n, where E is the electric field and n is the neutral density, behind the shock even though there is continuity of current. Note also that the emission intensities near both the cathode and the anode show no discernible change in intensity, confirming that under these operating parameters the discharge current changes little. These observations are correlated with an observed sharp decrease of the reduced electric field at the shock arrival time as measured by electrical probes [6]. The decrease in optical emission to practically zero intensity behind the shock front indicates a reduction of electron impact excitation and therefore also of ionization. As already observed from the ICCD images of the cathode and anode glow, the discharge current decreased only moderately during the time when the shock passed through the length of the positive column discharge tube for anode to cathode propagation. It even showed a small temporary increase for shock propagation in the direction from cathode to anode. The decrease of electronic excitation and ionization could be explained by the large increase of neutral density behind the shock front and therefore a decrease of E/n. However, the decrease of E/n with the increase in neutral density will also reduce the electron drift velocity. Therefore, discharge current continuity requires an increase of electron density, compensating drift velocity decrease, by a factor of 2 for the Mach 1.7 shock waves. The observed sharp drop in the local electric field propagating with the shock front indicated a local region of enhanced conductivity [6]. This abrupt change in electric field (requires net space charge to satisfy Poisson's equation) suggested the formation of a triple- or quadruple space charge layer connected with the shock front. The high electric fields in this very localized space charge region, ahead of the shock front, can then lead to local (dimension determined by the plasma Debye length) excitation and ionization that can provide the excess electron

density. The calculated electron density decay in an equivalent unperturbed positive column discharge was estimated to be at most 20% during a time equal to the shock traversal time.

The optical and electrical measurements gave a self-consistent picture of the plasma-shock wave interactions and the new measurements reported here provide evidence for the presence of strong excitation (and ionization) enhancement in a very narrow region propagating with the shock wave.

Under the conditions of the discharge (5 Torr, 50-100mA), the upstream neutral gas mean free path (temperature corrected) is 0.005cm and the estimated Debye length for the largest current is 0.01cm [6]. Assuming that the increase in optical emission will occur over the Debye length connected with the plasma conditions of the passing shock front, it will have a width of less than 0.3 mm. The spatial resolution requires that the full width of the discharge be within the depth of field of the photomultiplier optics. Taking a discharge diameter of 4 cm, on the outer limits of the diameter of the discharge, the optics used (f number 30, 90 mm focal length) will allow a resolution of only 1.7 mm (or blur disc diameter)[7]. A resolution of 0.1 mm is possible over a depth of field of 2.4 mm only. The combined effects of short radiation enhancement time and insufficient spatial resolution will broaden the pulse width of a shock induced enhanced optical radiation pulse and reduce its amplitude, making its detection difficult. These limitations may have been responsible for our inability to detect the expected electron impact excitation enhancement in C to B emission.

In order to improve our plasma emission detection sensitivity, we have measured the 2-0 vibrational transition of the $B^3\Pi_g - A^3\Sigma_u^+$ first positive band, which has a radiative

lifetime of 8.46 μs [8]. This longer lifetime along with the lower excitation energy level compared to the $C^3\Pi_u$ state was expected to give a better chance to observe the enhanced emission peak at the shock front. The B state can also be populated by cascading from three other states. The experimental setup, except for the spectral filter and a 3 cm diameter discharge tube with electrodes conformal with the glass wall, was identical to the one used previously [6]. This discharge geometry permits shock wave propagation measurements with the discharge polarity reversed with minimal modification of the test setup. The tube diameter was 3 cm diameter vs. 5 cm in the previously reported measurements [6], and at 3 Torr, the Mach number is about the same than in the previous measurements (Mach 1.76) using 100 Joules spark gap energy input. The narrower tube diameter and lower pressure also results in increased electron losses to the wall in this diffusion-dominated discharge so the electron mean energy is slightly higher than in the discharge of our previous report[6]. The optical observation point was 118 mm from the electrode closer to the spark gap and the distance between the electrodes was 180 mm. Fig. 2a shows the discharge voltage, current and 775.4 nm emission for a shock wave propagation from cathode to anode, fig.2b from anode to cathode, in both cases for a DC current of 20 mA at 3 Torr. The laser photo deflection markings of the shock front arrivals[6] in the 775.4 nm emission diagrams are for the physical location of the photomultiplier. The time period during which the shock wave traverses the discharge is indicated by the vertical dashed lines. As observed previously, the discharge voltage decreases and the current increases by 10% for about 100 μs for cathode to anode shock propagation direction, for the opposite propagation direction the voltage increases and the current decreases immediately. Again as previously observed, locally at the

photomultiplier observation point the light intensity increases when the shock wave enters the discharge for cathode to anode propagation and decreases for the opposite propagation direction. The electrical as well as the optical effects, before arrival of the shock at the observation point, are caused by the global electrical circuit response to the propagating shock wave, as described previously [6]. The global voltage and current perturbations in this smaller diameter, lower pressure discharge are larger than for the previous measurements [6]. A sharp and pronounced peak of 775.4 nm emission is observed when the shock wave passes through the observation region for both propagation directions. The emission peaks have a rise time of 2 μs and a decay time of about 40 μs. This long decay is in contrast to the 337.1 nm emission observed previously, which decays within less than 2 μs to practically zero intensity in conjunction with the fast increase in neutral density behind the shock. The long decay time is probably caused by the heavy particle collision induced excitation[9] of the B state due to the reaction $N_2(A^3\Sigma_u^+)+N_2(X^1\Sigma_g^+,v\geq5) \rightarrow N_2(B^3\Pi_g)+N_2(X^1\Sigma_g^+)$. (Both the $A^3\Sigma_u^+$ state and the vibrationally excited ground state have long life times).

The rapid rise in intensities of the 775.4 nm emission is an indicator of a large increase in electronic excitation rate connected with the shock wave induced very local increase in E/n value (or electronic energy distribution function). Due to the limitations of the optical system mentioned above, the temporal width of the rising portion of the measured 775.4 nm radiation pulses, which corresponds to the apparent duration of the shock wave generated local increase in E/n pulses, is much longer than the actual width of these radiation pulses and also the duration of the increased electronic excitation. For the same reason, the amplitudes of the measured pulses are much smaller than the actual radiation

amplitudes. For this positive column discharge [6], which runs at E/n ≈ 45 Td (1 Td= 1×10^{-17} V cm^{-1}), the observed $B^3\Pi_g - A^3\Sigma_u^+$ intensity jumps by at least 20% compared to the steady state in 2 μs. This requires a rate of change of the electron impact excitation by a factor of 10^5 indicating that the E/n increases [10] from 45 Td to > 240Td. The decay of the 775.4 nm radiation is strictly due to the population transfer from long-lived states after the short period of direct electron impact excitation enhancement; no such long decay was observed with the 337.1 nm radiation since the C state is populated primarily by direct electron impact.

In fig.3 the emission signals from the C to B and B to A states are compared. The photomultiplier output traces are aligned such that the signal amplitudes before arrival of the shock wave are about equal on the plot. The rise of the 775.4 nm signal corresponds to the arrival of the shock wave, and the decay of the 337.1 nm signal to the departure of the shock wave from the observation point. Due to the limitations in spatial resolution discussed above, the half width between the two signals is about 2 μs, which would correspond to a width of the shock wave of ≈ 1 mm at a velocity of Mach 1.76. As discussed above, the actual width is probably more than an order of magnitude smaller.

The decay of the discharge current follows an exponential function. While this dependence usually indicates ambipolar diffusion decay to the wall, the decay time constant is smaller than expected from a plasma with an estimated electron temperature of about 0.3 eV at the elevated pressure after the shock. We may assume that some of the charge carriers leave through the ends of the discharge since in this experiment, unlike in a conventional pulsed afterglow, there is still an applied electric field. However the E/n is much reduced and too

low for efficient ionization. Therefore, even with reduced drift velocity, the current to the discharge electrodes still will cause additional plasma loss.

The observed B to A emission enhancements show that the postulated [6], triple or quadruple space-charge layer connected with a shock wave propagating in non-equilibrium plasmas can induce strong local electronic excitation. We are presently investigating the consequence of the increase in local E/n on ionization enhancement, and also the local Joule heating that could be generated, at or near the shock front, by such an ionization enhancement produced by the shock induced space-charge layer formation in a nonequilibrium plasma.

References

1. G.I.Mishin, A.P.Bedin, N.I.Yushchenkova, G.E.Skvortsov, A.P.Ryazin, Sov.Phys. Tech.Phys. 26, 1363 (1981).
2. I.V.Basargin, G.I.Mishin, Sov.Tech. Phys.Lett. 11, 85 (1985)
3. A.Yu. Gridin, A.I..Klimov and N.E. Molevich, Sov. Phys. Tech. Phys. 38, 238 (1993).
4. P.A.Voinovich, A.P.Ershov, S.E.Ponomareva, V.M.Shibkov, High Temp. 29, 468 (1990)
5. Y.Z. Ionikh, N. V. Chernysheva, A. V. Meshchanov, A. P. Yalin and R.B. Miles, Phys. Lett. A 259, 387 (1999).
6. P. Bletzinger, B.N. Ganguly and A. Garscadden, Phys. Plasmas 7, 4341 (2000).
7. G.Franke ," Physical Optics in Photography" (Focal Press, London, 1966) p31-32
8. L.G.Piper, J. Chem. Phys. 91, 864 (1989).
9. L.G.Piper, K.W.Holtzclaw, and B.D. Green, J. Chem. Phys. 90, 5337 (1989).
10. K.Behringer and U.Fantz, J.Phys. D 27, 2128 (1994).
11. J.Loureiro and C.M.Ferreira, J.Phys. D 22, 67 (1989).

Figure Captions

Figure 1: ICCD camera images of the positive column light emission response of a N_2 discharge (5 Torr, 60 mA discharge current, 1.2μs exposure time, blue filter, tube diameter 5 cm) to a shock wave entering from the lhs of the photographs. The progression of the shock wave from cathode to anode is approximately indicated by the dashed line.

Figure 2a: Discharge voltage, current and 775.4 nm emission in a 3 Torr, 20 mA discharge in N_2 for a shock propagating from cathode to anode. A laser photodeflection signal for the location of the photomultiplier is shown in the 775.4 nm emission diagram. The time during which the shock traverses the discharge is indicated. (Photomultiplier intensity increases downwards).

Figure 2b: Same as figure 2a but for anode to cathode shock propagation.

Figure 3: Comparison of 337.1 nm and 775.4 nm emission signals for the same conditions as in figure 2a. The scales for each signal are adjusted such that the signal amplitudes before arrival of the shock are equal. The 775.4 emission increase correlates with the arrival of the shock wave at the observation point, the 337.1 emission decrease with the departure. The vertical markers indicate the time difference between the enhanced excitation (B-A), increased E/n signal and the signal decrease (C-B) caused by the density jump .

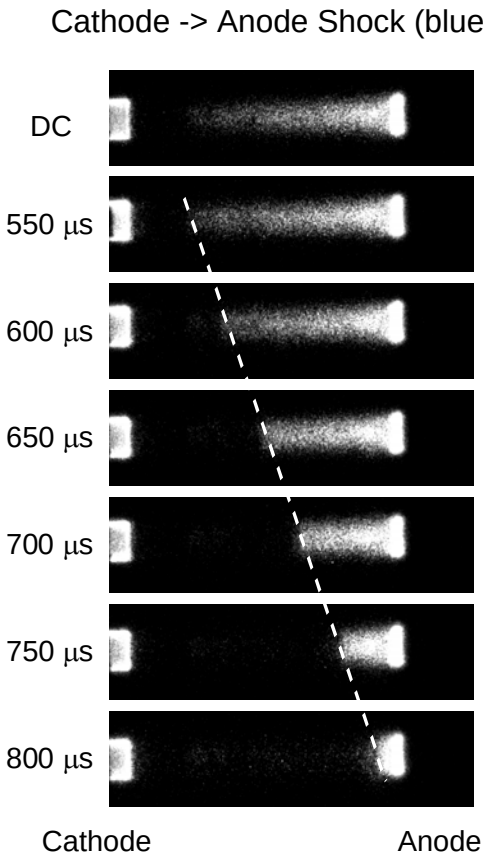
Cathode -> Anode Shock (blue filter)
DC
550 μs
600 μs
650 μs
700 μs
750 μs
800 μs
Cathode
Anode

Figure 1

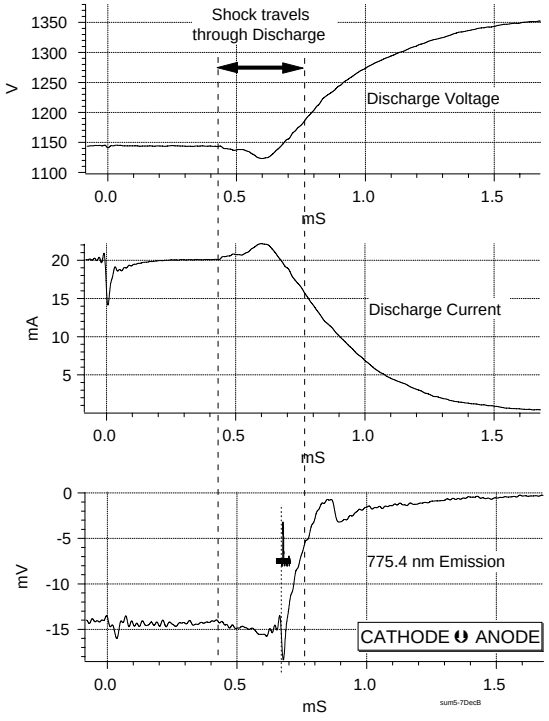
Shock travels
through Discharge
Discharge Voltage
V
1350
1300
1250
1200
1150
1100
0.0
0.5
1.0
1.5
mS
Discharge Current
mA
20
15
10
5
775.4 nm Emission
mV
0
-5
-10
-15
CATHODE
ANODE
sum5-7DecB

Figure 2a

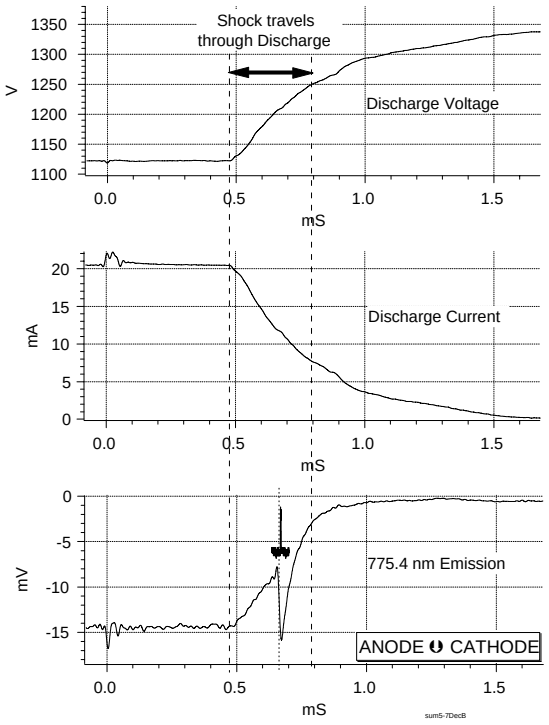
Shock travels
through Discharge
Discharge Voltage
V
1350
1300
1250
1200
1150
1100
0.0
0.5
1.0
1.5
mS
Discharge Current
mA
20
15
10
5
0
775.4 nm Emission
mV
0
-5
-10
-15
ANODE CATHODE
sum5-7DecB

Figure 2b

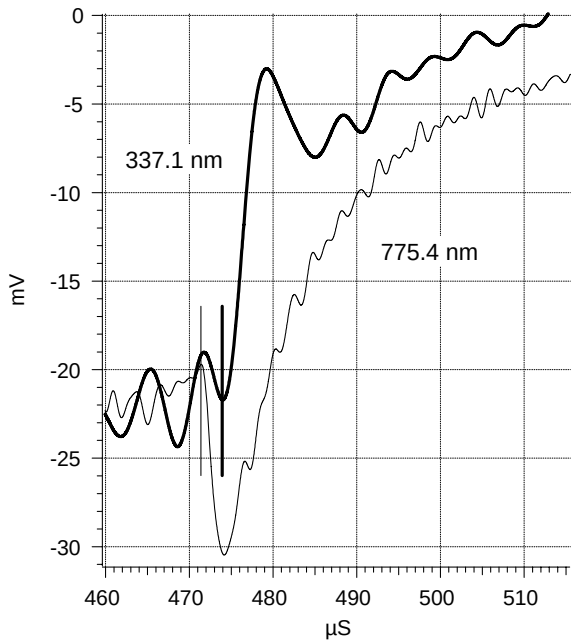

Figure 3

3. Shock Wave Propagation in a Dielectric Barrier Discharge

The effect of plasmas on shock waves has been investigated extensively for many years [1-14]. Many of the experiments have been performed with shock waves launched by an electrically pulsed discharge driven shock and the shock wave is propagated into a tube where a stationary plasma was generated. It was observed that the neutral gas density gradient of a shock wave decreased in the plasma and that the velocity of the shock wave increased compared to the values in the neutral gas. Since the stationary self-sustained plasma also causes an increase in neutral gas temperature, at least part of these effects can be produced by axial or radial temperature gradients in the volume of the plasma itself or at the plasma boundaries. However, at lower gas pressures and in non-equilibrium plasmas (average electron energy much larger than average ion energy), electrical effects and associated localized gas heating closely connected with the propagating shock wave in the plasma can also cause a reduction of the shock wave gradient and an increase of the shock wave velocity [12]. These electrical effects are caused by strong electrical double layers and manifest themselves with sharply increased, very localized optical excitation levels, a local increase in the electrical field and a large local increase in electron density, in addition to the shock wave broadening and velocity increase. All of these transient, local perturbations appear at exactly the location of the shock front and travel with the propagating shock wave. The magnitude of these effects increases with increasing Mach number and also with increasing reduced electric field E/n (where E electric field, n neutral density). Experiments have been mostly in nitrogen plasma. The plasma used in the previously reported experiments [10,11,12] was a low pressure unconstricted DC glow

discharge, which in N_2 is limited to pressures well below 100 Torr with current densities of less than 15 mA/cm^2 (more typically 1.5 to 3 mA/cm^2) with E/n in the range of 40 to 60 Townsend (Td, 1 Td = 1x10^{-17} Vcm^2). If the plasma effect for flow control is to be applied at higher pressures, other plasma generating techniques have to be utilized without, however, losing the non-equilibrium nature of the plasma. Also, as the strengths of the double layer effects increase with E/n, a plasma with a much higher value of E/n is desirable. A dielectric barrier discharge satisfies both of these requirements.

The dielectric barrier discharge (DBD) used consisted of a Pyrex discharge tube of 3 cm diameter with semicircular, 10 cm long external copper electrodes (Fig. 1). As in previous experiments[10,11,12] using a DC discharge, the shock wave was generated at one end by an electrical pulse discharge with electrical energy inputs into the spark gap of up to 500 Joules. The density jump generated by the propagating shock wave was measured by laser photodeflection at two locations, which allowed the determination of the average shock wave velocity between the photodeflection laser beam locations. The photodeflection signal is proportional to the derivative of the propagating density jump such that the width of this signal is a measure of the neutral density gradient [15]. The DBD circuit shorted out the high voltage electrode using a high speed, high voltage semiconductor switch with a switching time of about 20 ns or less. This electrode was charged with a 10 kOhm charging resistor. This arrangement allowed for grounding of one side of the high voltage switch as well as one of the DBD electrodes. The charging circuit and high voltage switch could provide variable pulse repetition rates up to 30 kHz at voltages up to 12 kV, the pulse width was determined by the electric charge on the electrodes and the characteristics of the plasma (Fig. 2). The flowing gas supply for the

discharge tube was measured by an electronic flow meter and the pressure was regulated by a downstream flow controller; a flow rate of 100 sccm of nitrogen was used.

An example of the discharge voltage and current at a pressure of 50 Torr in N_2 is shown in Fig. 2. Also shown is the current at 250 Torr, where there was no electrical discharge, which represents the displacement current into the capacitance of the circuit. The difference of the current at 50 Torr and the current at 250 Torr represents the current into just the discharge at 50 Torr. The current into the discharge is delayed until breakdown of the gas; in this example almost 10 ns after the switch closes. At that time the voltage across the discharge has already decreased, the gas discharge will be operated with a somewhat reduced voltage. The relationships between discharge operating voltage, gas pressure, pulse rise time and pulse current are complex; an example of a discharge in a gas mixture was published previously [16]. A consequence of using a fast switch is the large current contribution of the displacement current. In this example the total of the circuit and electrode capacitances is about 22 pF and even at a repetition rate of 30 kHz the average power into the discharge, calculated with the net current into the discharge as shown in Fig. 2, is less than 3 Watts. This of course also means that there will be very little heating of the neutral gas. At a pulse repetition rate of 30 kHz and a pulse width of 20 ns the duty cycle is 1.5×10^{-3}; the peak pulse power is 20 kW. The low average power into this discharge therefore makes it very unlikely that the observed effects on the shock wave such as an increase in velocity and shock wave broadening are caused by the upstream pre-existing thermal gradients. Also note that the major thermal gradient for the volume of the DBD is in a direction orthogonal to the tube axis from one electrode to the

other with the maximum temperature gradient close to the switched electrode, unlike the radial temperature gradient in a positive column discharge. A control experiment was performed measuring the rotational temperature in the volume using the second positive band, C-B (0, 3), emission of molecular nitrogen. The rotational spectra were obtained from spectral scans time averaged over several minutes. Within the margin of error there was little increase of rotational temperature above room temperature at pulse repetition rates to 30 kHz, as shown in Fig. 3. Temperature gradients at the plasma boundaries therefore will be small. Following Raizer [17] an estimate of the temperature rise in our 10cm long, 3 cm diameter N_2 discharge for a 3 W average power deposition results in a temperature rise of 30 K, which is close to the measured rotational temperature rise.

The influence of the DBD on a propagating shock wave is shown in Fig. 4 for a discharge in 30 Torr of N_2 and a discharge voltage of 10 kV. The shock wave pulse is not synchronized with the discharge pulses and as shown in Fig 4, the discharge pulses are positioned randomly in time in relation to the position of the shock wave and are not occurring at the same time as when the shock wave passes through the photodeflection laser beam locations. The DBD causes similar decreases in the shock wave neutral density gradients as a dc glow discharge, the shock velocity increases and the shock wave broadens. Varying the discharge voltage the shock wave velocity is seen to increase linearly with the voltage (Fig. 5a), it also increases linearly with pulse repetition frequency (Fig. 5b). The shock wave broadening also increases and as shown in Fig. 6 it is also a linear function of both discharge voltage (Fig. 6a) and pulse repetition frequency (Fig. 6b). These measurements were also obtained at 30 Torr in N_2.

If we assume that the shock wave velocity increase is caused by the shock wave passing through an upstream axial temperature gradient at the discharge boundary, we can calculate the jump in upstream gas temperature required to produce the measured velocity increase. As an example, taking the velocity increase in Fig. 5a) from 448 m/sec with no discharge to 510 m/sec for a discharge voltage of 10 kV, using the equations derived by Aleksandrov et al [18], an upstream gas temperature gradient of more than 104 K is required. Clearly this is significantly larger than the small rotational temperature increase indicated in Fig. 3.

One important question for the effect of plasmas on shock waves is the interaction distance required for the observable modification of the shock wave properties. Since the DBD can operate at higher pressure, a measurement was performed at 70 Torr, where the (optical) boundary of the discharge was clearly defined and the edge of the plasma was aligned with the edge of the external electrodes. In Fig. 7 a comparison is shown of the photodeflection at a location 12 mm before the edge of the plasma with the photodeflection 10.5 mm into the discharge with the discharge off and when the DBD is operated at 20 kHz repetition rate and 10 kV. The photodeflection signal before the discharge (left peaks) is completely unaffected by the discharge, the signals for off and on conditions are identical. Inside the DBD the photodeflection signal shows both an increase in velocity and shock broadening with the discharge on, indicating that the plasma is effective in modifying the shock wave already within 10.5 mm distance or 25 μs propagation time into the discharge. Applying the equations for an upstream gas temperature gradient induced shock wave velocity increase [18] for this case, a required pre-existing upstream gas temperature increase of 79 K was calculated; again

considerably higher than the calculated or measured temperature rise from the global power deposition into the discharge. For a constant applied pulsed voltage, the shock wave broadening decreases with increasing pressure.

The DBD is considerably more efficient in broadening shock waves than a DC glow discharge. This is shown in Fig. 8, where equal amounts of broadening are plotted (a) for both the DBD (versus repetition rate, bottom abscissa) and a DC glow discharge (versus discharge current, top abscissa). Using this data, the resulting average power for the DBD and the power into the DC discharge are calculated for these broadening values and plotted in the Fig. 8b. This comparison shows the DBD to be almost an order of magnitude more efficient in producing the same amount of shock wave broadening. Considering that for this DBD power calculation the contribution of the displacement current was not subtracted, the power into the DBD is a maximum value and the actual input power efficiency of the DBD for modifying shock wave broadening is even larger compared to the dc discharge.

The shock wave initiation and propagation are not synchronized with the DBD pulses; because of the low duty cycle in these experiments, the shock is typically propagating in the discharge afterglow. Even in the case where the broadening was measured close to the discharge boundary, and particularly at the lower pulse repetition rates, the shock wave measurements showed velocity increases and broadening even when the probability of the shock wave having been exposed to a discharge pulse was very low. The question then arises on how the shock wave is affected in the period between discharge pulses. These observations require that the time period between the pulsed discharges, namely

the discharge afterglow, must also be effective in producing strong double layers which can modify the shock wave.

We have previously made measurements of the time and spatially resolved electron density using a microwave interferometer and of the optical emission using a photomultiplier with imaging optics and spectral filter in DC glow discharges [12]. When in these measurements the shock wave velocity was increased, the discharge current decrease at the time of entrance of the shock wave into the plasma became more rapid until, above a certain Mach number, the current decreased to near zero. The electron density jump, measured using the microwave interferometer, correlated with the shock wave increased in amplitude with increasing shock wave Mach number. An example of such measurements is shown in Fig. 9 for a 3 Torr discharge with 8.5 mA/cm^2 current density, and for two different Mach number shock wave propagation through the positive column. Fig. 9 shows voltage (9a), current (9b) and electron density (9c) for two shock velocities. Note that the electron density jump is greater for Mach 2.7 compared to Mach 1.74. Also for the Mach 2.7 shock wave propagation, this local electron density increase happened even when the discharge current already had decreased by a factor of three from its steady state value at the time when the electron density jump was observed. Similarly, when the shock wave passes the observation point, the 775.4 nm B-A light emission jump increased in intensity with increasing Mach number and it took place after the circuit current was almost zero. Fig. 10c shows the 775.4 nm light emission at two fiber optic coupled photomultiplier observation positions, separated by 13.5 cm, inside the 3 Torr positive column discharge with 1.7 mA/cm^2 current density for a shock wave velocity of 992 m/sec. Also shown are the shock propagation induced changes of the

discharge voltage (Fig. 10a) and the discharge current (Fig. 10b). Strong increases in local B-A emission pulses are observed after the discharge current has decreased to zero, their amplitudes decreasing with increasing delay relative to the current decrease [19]. These discharge afterglow effects were further verified by shorting out the discharge voltage, with the 20 ns rise time high voltage switch, before shock arrival at the observation points and measuring the B-A light emission amplitudes in the afterglow. These plasma-shock interaction results are consistent with the properties of the electron energy relaxation in the pure N_2 afterglow. The change of the 775.4 nm emission decay in the normally switched off discharge with a decay constant of about 200-300 μs to a rapid decay after the shock wave passes the observation point (decay constant about 12 μs) indicates a large increase in the electron diffusion loss which can be explained by a shock wave caused shift in the electron energy distribution[12].

The afterglow in pure N_2 has been the subject of numerous investigations. Recent work has concentrated on the decay of the electron density and excited states [20, 21] and these investigations show lifetimes of both the relevant excited states and decay times of the electron density to be in the order of msec. The electron density decay is dominated for 10^{-5} to 10^{-4} s at 2 Torr and 10^{-5} to 10^{-3} s at 10 Torr by the slow ambipolar diffusion, before switching to free diffusion [22]. For the electron energy distribution, after a rapid initial loss of high energy electrons, "for times $\geq 10^{-6}$ s the electron energy distribution function attains a quasi-stationary state" (for the afterglow of a 433 MHz, 3.3 Torr, R=1.9 cm discharge) [19].

These long electron energy decay times then are apparently sufficient to allow the shock induced double layer effects to influence the shock waves for at least 100's of μs after

cessation of the excitation by an external applied electrical field and especially after excitation with a high E/n short pulsed dielectric barrier discharge.

While the parameter range of neutral gas pressures and electrical excitation has not been fully explored for these effects, it is apparent that the electrical double layer formation responsible for the shock wave modification as suggested in our previous work [12] is functional in a DBD. In the DBD the shock generates a large local electric field extending over several Debye lengths and produce local axial temperature gradients linked with the propagating shock wave. For any technical applications, for example for hypervelocity vehicles or general high speed flow control, the DBD appears more versatile than a glow discharge, offering many possible electrode and discharge configurations .

References:

[1] O.W. Greenberg, H. K. Sen, and Y. M. Treve, Phys. Fluids. 3, 379 (1960)

[2] M. Y. Jaffrin, Phys. Fluids 8, 606 (1965)

[3] M.A. Liberman and A. L. Velikovich, Physics of Shock Waves in Gases and Plasmas (Springer, New York, 1985), pp 91-128.

[4] G.I.Mishin, A.P.Bedin, N.I.Yushchenkova, G.E.Skvortsov, A.P.Ryazin, Sov.Phys.Tech.Phys. 26, 1363 (1981).

[5] A.I.Klimov, A.N.Koblev, G.I.Mishin, Yu.L.Serov, I.P.Yavor, Sov.Phys.Tech.Phys. Lett. 8, 192 (1982).

[6] I.V.Basargin, G.I.Mishin, Sov.Tech. Phys.Lett. 11, 85 (1985)

[7] A.Yu. Gridin, A.I..Klimov and N.E. Molevich, Sov. Phys. Tech. Phys. 38, 238 (1993).

[8] P.A.Voinovich, A.P.Ershov, S.E.Ponomareva, V.M.Shibkov, High Temp. 29, 468 (1990)

[9] S.A.Bystrov, I.S.Zaslonko, Yu.K.Mukoseav, F.V.Shugaev, Sov.Phys.Dokl. 35, 39 (1990)

[10] P.Bletzinger and B.N.Ganguly, Phys. Lett. A 258, 342 (1999)

[11] P. Bletzinger, B.N. Ganguly and A. Garscadden, Phys. Plasmas 7, 4341 (2000)

[12] P. Bletzinger, B.N. Ganguly and A. Garscadden, Phys. Rev E67, 047401 (2003)

[13] S.O. Macheret, Y. Z. Ionikh, N. V. Chemysheva, A. P. Yalin, L. Martinelli, and R. B. Miles, Phys. Fluids 13, 2693 (2001)

[14] P.Bletzinger, B.N.Ganguly, D Van Wie and A.Garscadden, J.Phys.D:Appl.Phys.38, R33-R57

[15] J.H.Kiefer, R.W.Lutz, J.Chem.Phys. 44, 658 (1966)

[16] P. Bletzinger and B. N. Ganguly, J. Phys. D: Appl. Phys.**36**, 1550 (2003)

[17] Yu.P.Raizer, "Gas discharge physics", Springer, New York 1991

[18] A. F. Aleksandrov, N.G. Vidyakin, V.A. Lakutin, M.G. Skvortsov, I.B. Timofeev and V.A. Chernikov, Sov. Phys. Tech. Phys. 31, 468 (1986)

[19] At faster shock wave velocities the stronger shock pulse required will cause some photoionizing radiation to leak into the volume of the discharge and temporarily increase discharge conductivity and light emission before the shock wave arrives at the discharge

[20] N. Sadeghi, C. Foissac, and P. Supiot, J. Phys. D: Appl. Phys. **34**, 1779 (2001).

[21] V. Guerra, F. M. Dias, J Loureiro, P. Sa, P Supiot, C. Dupret, T. Popov, IEEE Trans. Plasma Science 31, 542 (2003)

[22] V.Guerra, P.A.Sa and J.Loureiro, Phys.Rev.E, 63, 046404-1 (2001)

Figure captions:

Fig. 1: Schematic of experiment.

Fig. 2: Voltage and current of DBD discharge at 50 and 250 Torr N_2. At 250 Torr there is no discharge and this displacement current can be subtracted from the total current (at 50 Torr) to obtain the net current into the discharge.

Fig. 3: Rotational temperature of DBD in N_2 as a function of repetition rate, N_2 20 Torr, 5 kV.

Fig. 4: Photodeflection signals from shockwave propagating through discharge tube. With no discharge and 2, 5 and 20 kHz discharge at 10 kV. N_2, 30 Torr. Oscilloscope traces are shifted vertically. Shock pulse and discharge pulse were not synchronized

Fig. 5 Shock wave velocity as a function of discharge voltage at 20 kHz(a) and as a function of pulse repetition frequency at 10 kV(b). N_2, 30 Torr.

Fig. 6: Shock wave broadening as measured from the width of the photodeflection signal as a function of discharge voltage at 20 kHz(a) and discharge pulse frequency at 10 kV(b). N_2, 30 Torr.

Fig. 7: Photodeflection signal in a 70 Torr N_2 discharge at two positions before and after discharge boundary. Pulse frequency 20 kHz at 10 kV discharge voltage. Insert shows location of laser beams for shock wave photodeflection measurements. Shock wave moves from right to left.

Fig. 8: Comparison of photodeflection signals for DC glow discharge and DBD. Figure 8a) shows broadening as a function of current for DC discharge and

pulse frequency for DBD, operated at 5 kV. Figure 8b) shows corresponding DC (right ordinate) or average DBD power (left ordinate) as function of DC current or DBD pulse frequency. Pressure for both discharges: 5 Torr, N_2.

Fig. 9: Discharge voltage (a), current (b) and microwave interferometer signal or electron density (c) for 3 Torr DC glow discharge and with two different Mach number shock waves.

Fig. 10: a) Discharge voltage change, b) current and c) 775.4 nm first N2 positive system band head amplitude at two photomultiplier positions at 3 Torr, 12 mA DC discharge in N_2 with shock wave at 992 m/s.

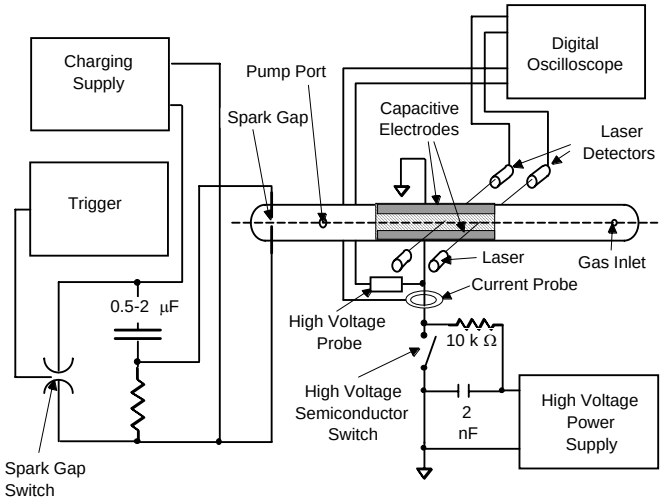
Charging Supply
Trigger
Digital Oscilloscope
Pump Port
Spark Gap
Capacitive Electrodes
Laser Detectors
Laser
Gas Inlet
Current Probe
0.5-2 μF
High Voltage Probe
10 k Ω
High Voltage Semiconductor Switch
2 nF
High Voltage Power Supply
Spark Gap Switch

Figure 1.

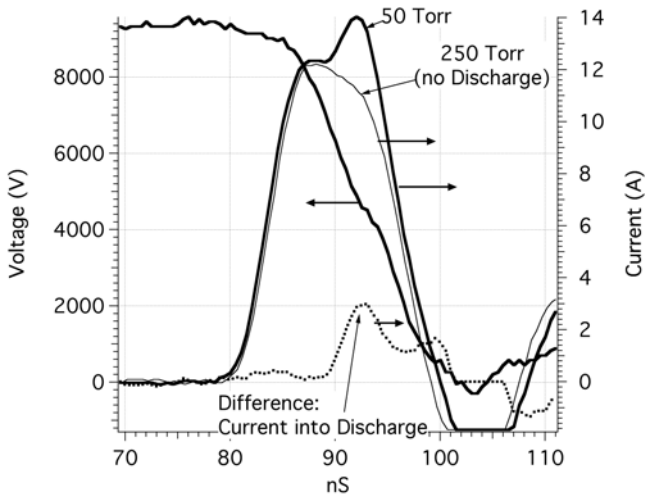
50 Torr
250 Torr
(no Discharge)
Difference:
Current into Discharge
Voltage (V)
Current (A)
nS
8000
6000
4000
2000
0
14
12
10
8
6
4
2
0
70
80
90
100
110

Figure 2.

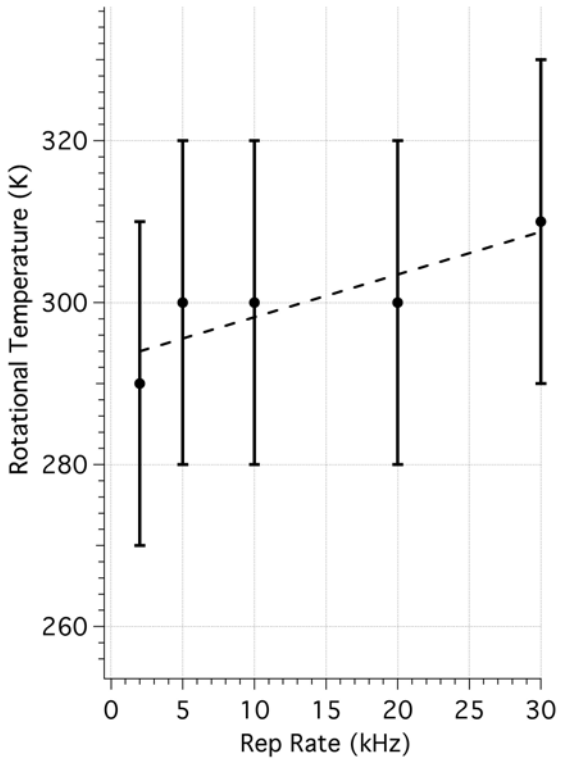
Rotational Temperature (K)
320
300
280
260
0
5
10
15
20
25
30
Rep Rate (kHz)

Figure 3.

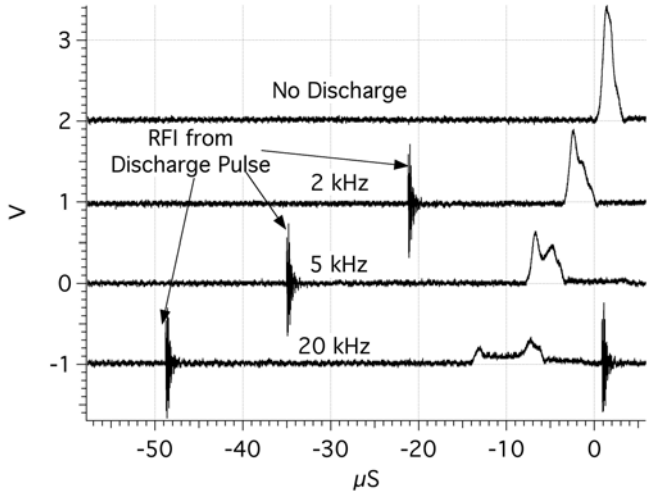
No Discharge
RFI from
Discharge Pulse
2 kHz
5 kHz
20 kHz
V
3
2
1
0
-1
-50
-40
-30
-20
-10
0
μS

Figure 4.

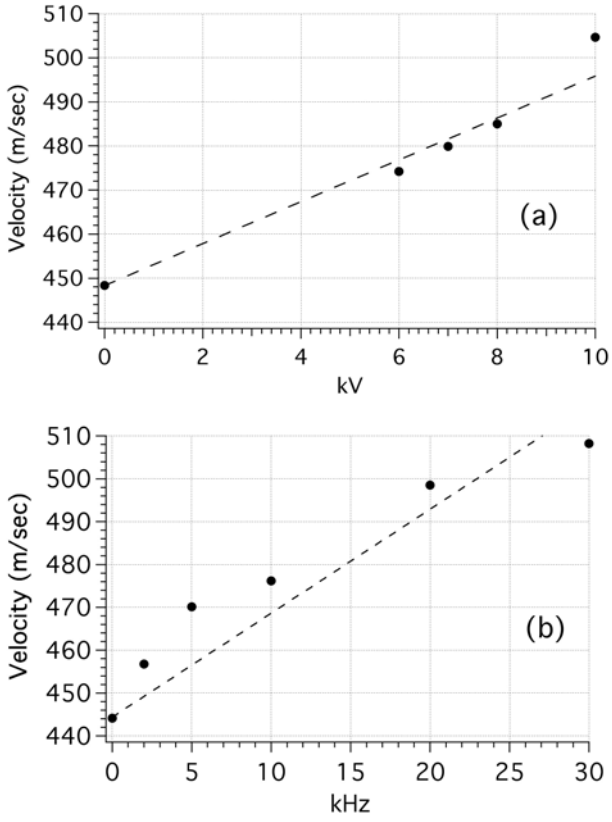
Velocity (m/sec)
510
500
490
480
470
460
450
440
0
2
4
6
8
10
kV
(a)
Velocity (m/sec)
510
500
490
480
470
460
450
440
0
5
10
15
20
25
30
kHz
(b)

Figure 5.

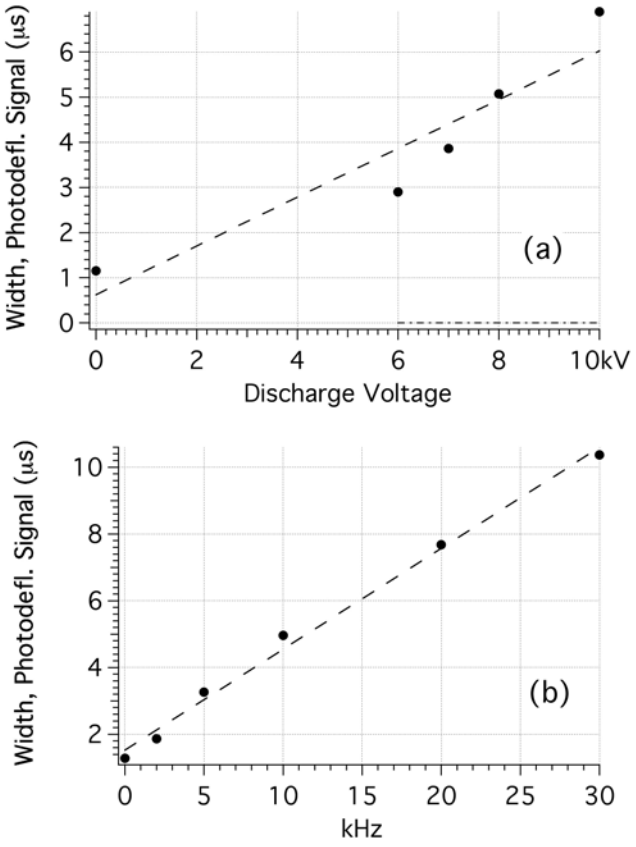
Width, Photodefl. Signal (μs)
0
1
2
3
4
5
6
(a)
0
2
4
6
8
10kV
Discharge Voltage
Width, Photodefl. Signal (μs)
2
4
6
8
10
(b)
0
5
10
15
20
25
30
kHz

Figure 6.

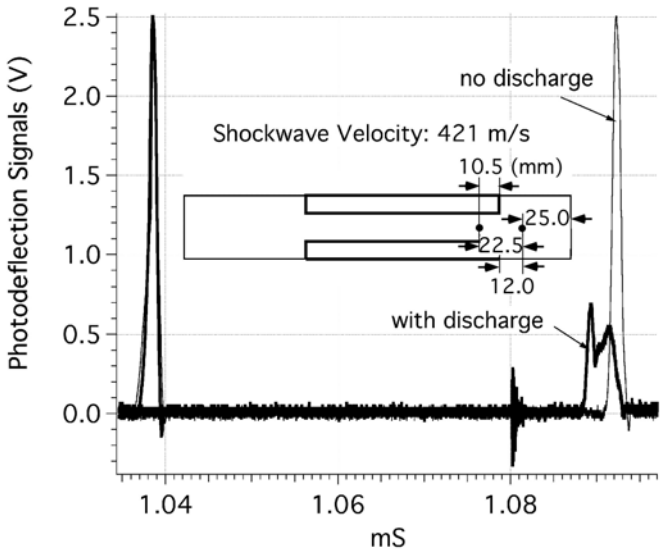
Photodeflection Signals (V)
2.5
2.0
1.5
1.0
0.5
0.0
1.04
1.06
1.08
mS
no discharge
Shockwave Velocity: 421 m/s
10.5 (mm)
25.0
22.5
12.0
with discharge

Figure 7.

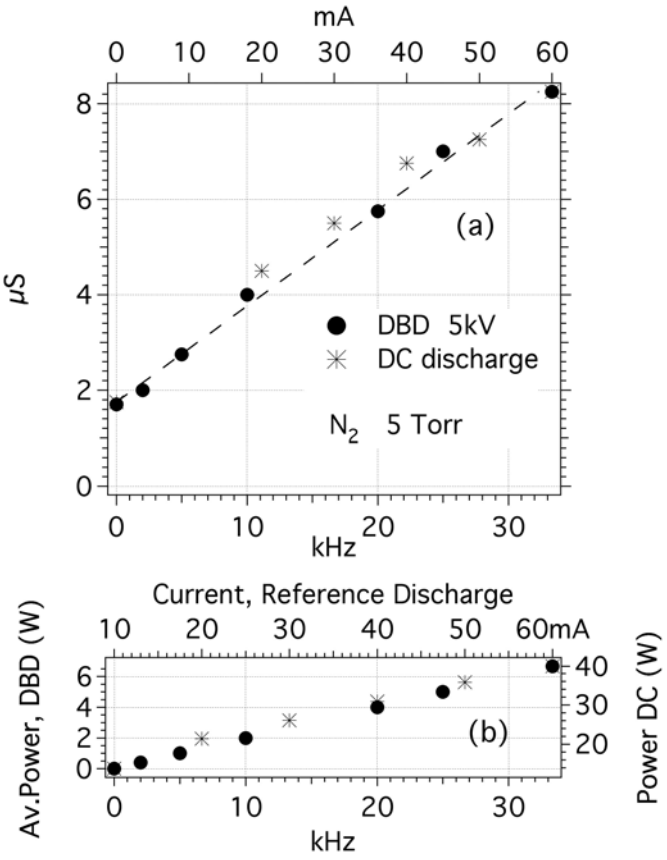
mA
0 10 20 30 40 50 60
8
6
4
2
0
μS
(a)
DBD 5kV
DC discharge
N2 5 Torr
0 10 20 30
kHz
Current, Reference Discharge
10 20 30 40 50 60mA
6
4
2
0
Av.Power, DBD (W)
40
30
20
Power DC (W)
(b)
0 10 20 30
kHz

Figure 8.

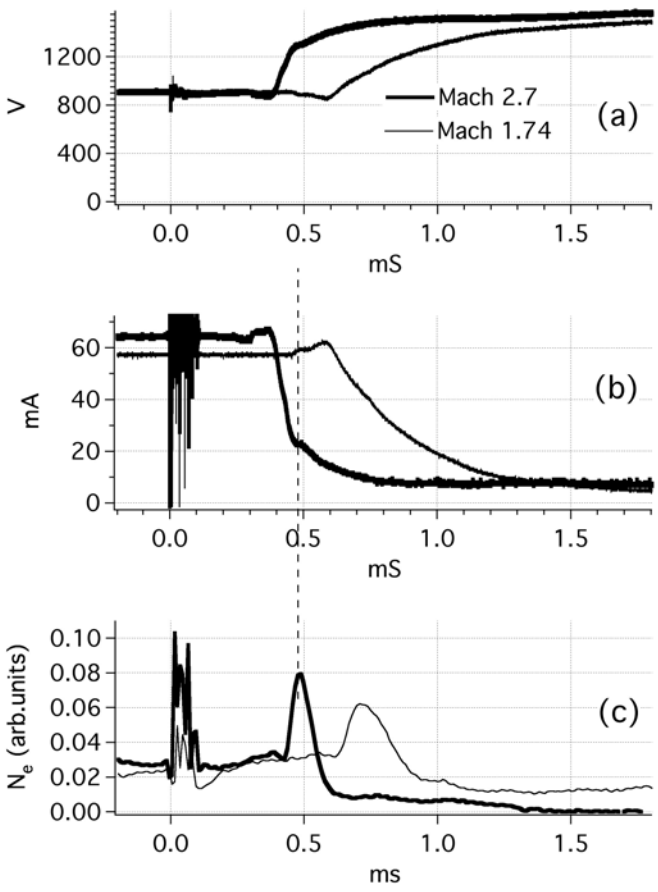
V
1200
800
400
0
Mach 2.7
Mach 1.74
(a)
0.0
0.5
1.0
1.5
mS
mA
60
40
20
0
(b)
mS
N_e (arb.units)
0.10
0.08
0.06
0.04
0.02
0.00
(c)
ms

Figure 9.

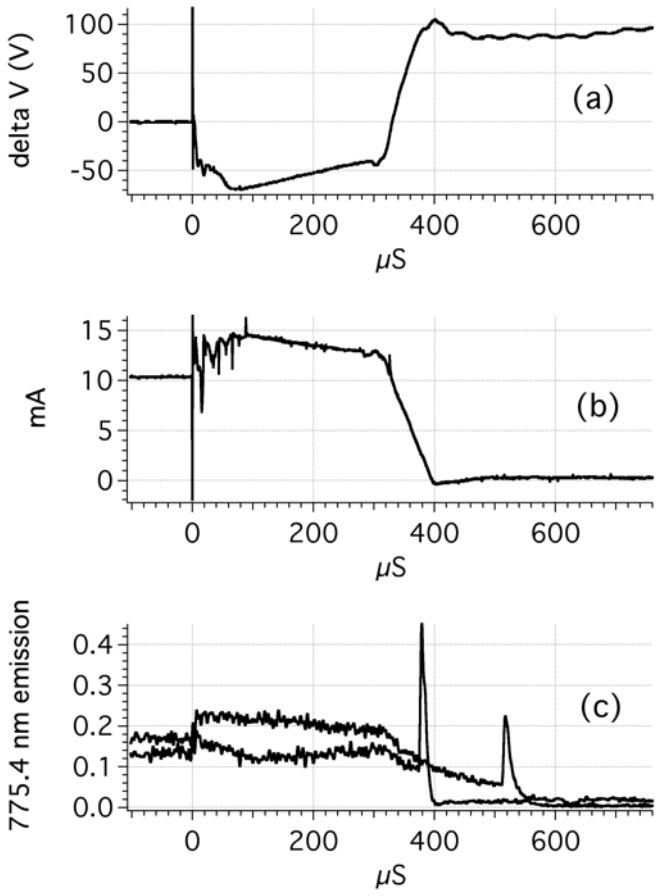
delta V (V)
100
50
0
-50
(a)
0
200
400
600
μS
mA
15
10
5
0
(b)
0
200
400
600
μS
775.4 nm emission
0.4
0.3
0.2
0.1
0.0
(c)
0
200
400
600
μS

Figure 10.